Solid state quantum memory for photons at telecommunication wavelengths

Björn Lauritzen,* Jiří Minář, Hugues de Riedmatten, Mikael Afzelius, Nicolas Sangouard, Christoph Simon, and Nicolas Gisin
Group of Applied Physics, University of Geneva, CH-1211 Geneva 4, Switzerland

We demonstrate experimentally a solid-state quantum memory for photons at telecommunication wavelengths. Weak light fields at the single photon level are stored for a time up to 600 ns in an Erbium-doped Y_2SiO_5 crystal at 2.6 K and retrieved on demand. The memory is based on photon echoes with controlled reversible inhomogeneous broadening. This is implemented with an external field gradient using the linear Stark effect.

PACS numbers: 03.67.Hk,42.50.Gy,42.50.Md

arXiv:0908.2348v1 [quant-ph] 17 Aug 2009

Quantum memories allowing the reversible transfer of quantum states between light and matter are an essential requirement in quantum information science [1]. They are, for example, a crucial resource for the implementation of quantum repeaters[2, 3, 4, 5], which are a potential solution to overcome the limited distance of quantum communication schemes due to losses in optical fibers. Several schemes have been proposed to implement photonic quantum memories [6, 7, 8, 9, 10, 11, 12]. Important progress has been made during the last few years, with proof of principle demonstrations in atomic gases [13, 14, 15, 16, 17, 18, 19, 20], single atoms in a cavity [21], and solid state systems [22]. For all these experiments the wavelength of the stored light was close to the visible range and thus not suited for direct use in optical telecom fibers. The ability to store and retrieve photons at telecommunication wavelengths (around 1550 nm) in a quantum memory would provide an important resource for long distance quantum communication. Such a quantum memory could easily be integrated in the fiber communication network. In combination with a photon pair source, it could provide a narrow band triggered single photon source adapted to long distance transmission. Moreover, quantum memories at telecommunication wavelengths are required for certain efficient quantum repeater architectures [5, 23, 24].

The implementation of a quantum memory at telecom wavelengths requires an atomic medium with an optical transition in the telecom range, involving a long lived state. The only candidate proposed so far is based on erbium doped solids, which have a transition around 1530nm between the ground state $^4I_{15/2}$ and the excited state $^4I_{13/2}$. These systems have been studied for spectroscopic properties [25, 26] and classical light storage [27, 28, 29]. However, photonic quantum storage in these materials is extremely challenging, because of the difficulties in the memory preparation using optical pumping techniques [30]. In this paper, we report an experiment of storage and retrieval of weak light fields at the single photon level in an erbium doped solid.

*Electronic address: bjorn.lauritzen@unige.ch

Rare-earth doped solids have an inhomogeneously broadened absorption line. Single photons can be mapped onto this optical transition, leading to single collective optical excitations [22]. During the storage, inhomogeneous dephasing will take place, preventing an efficient collective re-emission of the photon. This dephasing can be compensated for using photon echo techniques. The storage of quantum light (e.g. single photons) is however not possible using traditional photon echo techniques, such as two pulse photon echoes [31]. The main issue is that the application of the strong optical pulse (π-pulse) to induce the rephasing mechanism will lead to amplified spontaneous emission and reduce the fidelity of the storage to an unacceptable level [32]. A way to overcome this problem is to induce the rephasing of the atomic dipoles by generating and reversing an artificial inhomogeneous broadening. This scheme is known as Controlled Reversible Inhomogeneous Broadening (CRIB) [8, 9, 33, 34]. In rare-earth doped solids with a permanent dipole moment, this can be done with an electric field gradient using the linear Stark effect. The CRIB scheme was first demonstrated with bright optical pulses at 580 nm [33], in a Eu^{3+}:Y_2SiO_5 crystal. The phase of the stored light pulses was shown to be well preserved [35]. For these experiments, the storage and retrieval efficiency was of the order of $10^{-5} - 10^{-6}$. It has been dramatically improved in more recent experiments at 606 nm in Pr^{3+}:Y_2SiO_5 [36]. CRIB has also been demonstrated on a spin transition in a rubidium vapor [37]. Here, we report the first experimental demonstration of CRIB for light at telecommunication wavelengths at the single photon level.

In order to realize a CRIB experiment in a rare-earth doped solid, one first has to prepare a narrow absorption line within a large transparency window. The spectrum of this line is then broadened by an electric field gradient using the linear Stark effect to match the bandwidth of the photon to be stored. The incident photon is absorbed by the ions in the broadened line, and mapped into a single collective atomic excitation. During a time t each excited ion i will acquire a phase $\Delta_i t$ due to its shift in the absorption frequency $\omega_i = \omega_0 + \Delta_i$ from the central frequency ω_0. Switching the polarity of the field after a time $t = \tau$ will reverse the broadening ($\omega_i = \omega_0 - \Delta_i$)

and after another time τ the ions will be in phase again and re-emit the photon. In order to create the initial narrow absorption line, a population transfer between two ground states (in our case Zeeman states) using optical pumping via the excited state is used [30]. In case of imperfect optical pumping there will be population remaining in the excited state after the preparation sequence. An experimental issue arising when input pulses are at the single photon level is the fluorescence from these atoms left in the excited state during the preparation of the memory. If the depletion of this level is slow (as in rare-earth ions, with optical relaxation times T_1 usually in the range of 0.1 ms to 10 ms), this can lead to a high noise level from fluorescence that may blur the weak echo pulse. The problem is especially important for erbium doped solids, where T_1 is very long ($\approx$ 11 ms [25] in Er^{3+}:Y_2SiO_5). In our experiment, the population transfer is enhanced by stimulating ions from the excited state down to the short lived second ground state crystal field level using a second laser at 1545 nm (Fig. 1a) [30]. The application of this laser enhances the rate of depletion of the excited state and thus reduces the noise from fluorescence. Together with a suitable waiting time between the preparation and the light storage, it allows the realization of the scheme at the single photon level.

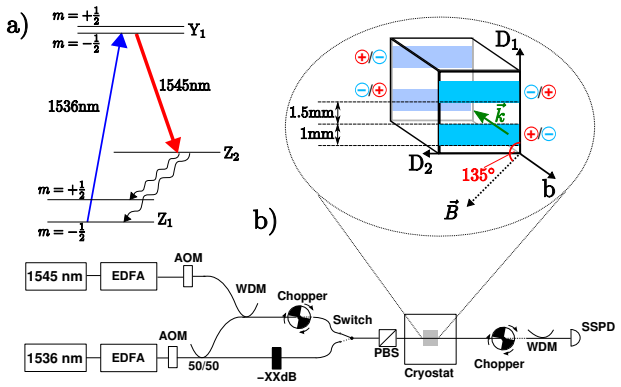

FIG. 1: (color online) (a) Level scheme of Er^{3+}:Y_2SiO_5. (b) Experimental setup: The pump laser (external cavity diode laser at 1536nm) is split into two paths, one for the preparation pulses and one for the weak pulses to be stored. Pulses are created with acousto-optical modulators (AOMs). In the preparation path, the stimulation laser (DFB laser diode at 1545nm+fiber amplifier) is added using a wavelength division multiplexer (WDM). The pulses to be stored are attenuated to the single photon level with a fiber attenuator. An optical switch allows to send either of them into the sample. In order to protect the detector (SSPD) and to avoid noise from a leakage of the optical switch, two mechanical choppers are used. The polarization of the light is aligned to maximize the absorption using the polarizing beam splitter (PBS). Inset: illustration of the crystal with electrodes, magnetic field and light propagation directions indicated.

Our memory consists of an Y_2SiO_5 crystal doped with erbium (10ppm) cooled to 2.6 K in a pulse tube cooler (Oxford Instruments). The crystal has three mutually perpendicular optical-extinction axes labelled D1, D2, and b. Its dimensions are 3.5 × 4 × 6mm along these axes. The magnetic field of B =1.5 mT used to induce the Zeeman splitting necessary for the memory preparation is provided by a permanent magnet outside the cryostat and is applied in the $D_1 - D_2$ plane at an angle of $\theta = 135°$ with respect to the D_1-axis [38] (Fig.1b). The light is travelling along b. The electrical field gradient for the Stark broadening is applied with four electrodes placed on the crystal in quadrupole configuration, as shown in Fig.1b and described in [39]. The induced broadening is proportional to the voltage U applied on the electrodes [39].

The experiment is divided into two parts: the preparation of the memory and the storage of the weak pulses (see Fig.1b). Each preparation sequence takes 120ms of optical pumping during which both the pump and the stimulation lasers are sent into the sample. The frequency of the pump laser is repeatedly swept to create a large transparency window into the inhomogeneously broadened absorption line. If the laser is blocked for a short time at the center of each sweep using an acousto-optical modulator (AOM), a narrow absorption feature is left at the center of the pit [30]. The time available to perform the memory protocol is given by the Zeeman lifetime of T_Z = 130ms [38] of the material. In order to deplete the excited state the laser at 1545nm is left on for 23.5ms after the pump pulses. Then the preparation path is closed and the detection path is opened using an optical switch and mechanical choppers. The storage sequence begins 86ms after the pump pulse, in order to avoid fluorescence from the excited atoms. It is composed of 8000 independent trials separated by 5μs. In each trial, a weak pulse of duration $\delta\tau$ is stored and retrieved. The initial peak is broadened with an electrical pulse before the absorption of each pulse. The polarity of the field is then inverted at a programable time after the storage, allowing for on demand read-out. The whole sequence is repeated at a rate of 3Hz. The weak output mode is detected using a superconducting single photon detector (SSPD) [40] with an efficiency of 7% and a low dark count rate of 10 ± 5Hz. The incident pulses are weak coherent states of light $|\alpha\rangle_L$ with a mean number of photons $\overline{n} = |\alpha|^2$. We determined $\overline{n}$ at the input of the cryostat by measuring the number of photons arriving at the SSPD (with the laser out of resonance), compensating for the transmission between the input of the cryostat and the detector (16%) and the efficiency of the latter.

We now describe the observation of CRIB photon echoes of weak pulses. As a first experiment, we sent pulses with $\overline{n}$ =10 and $\delta\tau$ = 200 ns into the sample. The polarity of the electric field ($U = \pm$ 50 V) was reversed directly after each pulse. Fig. 2 shows a time histogram of the photon counts detected after the crystal. The first peak corresponds to the input photons transmitted through the crystal. The second peak is the CRIB echo. It is clearly visible above the noise floor. Only a small fraction of the incident light is re-emitted

in the CRIB echo (about 0.25 %). The reasons for this low storage and retrieval efficiency and ways to improve it will be discussed in more detail below. As a consistency check, we verified that the echo disappears when the narrow absorption peak is not present (see blue open circles in Fig. 2). By reversing the electric field gradient at later times, it is possible to choose the retrieval time of the stored light. Fig. 3 shows the efficiency of the CRIB echo for different storage times. The signal was clearly visible up to a storage time of around 600 ns. The decay of the efficiency is due to the finite width of the initial (unbroadened) peak [11] (see below). The solid line is a fit assuming a gaussian shape for the absorption line, giving a decay time of 370 ns. Shorter pulses with $\delta\tau$ = 100 ns have also been stored (see the inset of Fig. 3) with a larger broadening (U = ± 70 V), leading to a larger time-bandwidth ratio, with however a reduced storage efficiency. Finally, we gradually lowered $\overline{n}$ by increasing the attenuation, for input pulses with $\delta\tau$=200 ns . The result is shown in Fig. 4a. Both the number of photons in the CRIB echo and the signal to noise ratio depend linearly on $\overline{n}$. This means that the efficiency and the noise are independent of $\overline{n}$. Fig. 4b shows the result of a measurement with - in quantum key distribution terminology - pseudo-single photons ($\overline{n}$ = 0.6 photons per pulse). In that case, the mean photon number in the CRIB echo at the output of the sample is 10^{-3}. For this measurement, we still obtain a signal to noise ratio of ∼3. The remaining noise floor may be due to residual fluorescence and leakage through the AOM creating the pulses to be stored.

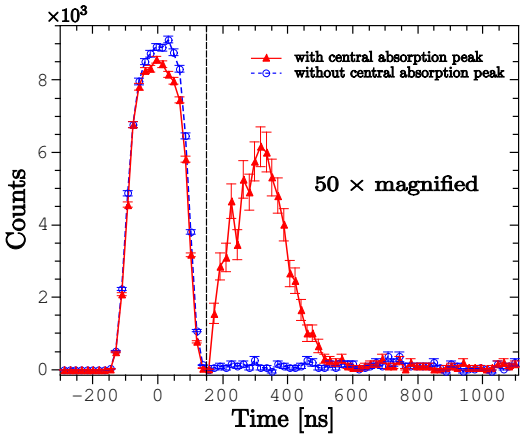

FIG. 2: (color online) CRIB measurement with (red triangles, solid line) and without (blue circles, dashed line) absorption peak, with $\overline{n}$ = 10 and $\delta\tau$ = 200 ns. The pulse on the left is the transmitted part of the incident photons. One can clearly see that the absorption is enhanced in the presence of a peak. The electric field (U=±50 V) was reversed just after the input pulse. Dark counts have been subtracted from the data. Integration time for both curves was 200s.

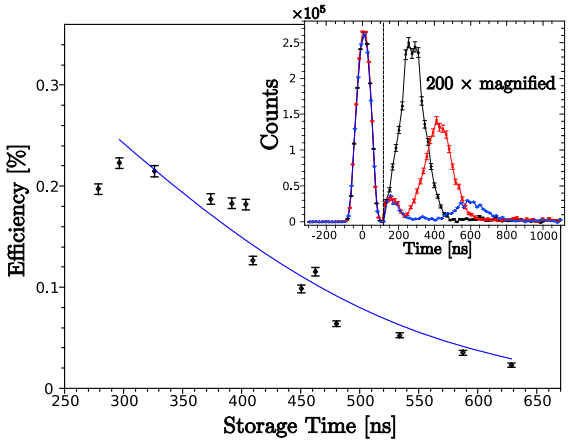

FIG. 3: (color online) Efficiency of the CRIB memory as a function of storage time, for input pulses with $\delta\tau$=200 ns , $\overline{n}$ = 10 and U = ±50 V. The error bars correspond to the statistical uncertainty of the measured photon numbers. The solid line is a gaussian fit (with the first point excluded). The inset shows CRIB echoes for three different switching times of the electrical field. For the inset curves, $\delta\tau$=100 ns, U=±70 V and the integration time is 500 s.

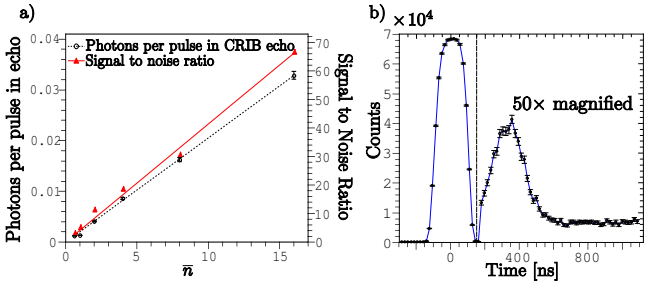

FIG. 4: (color online) (a) Number of photons in the CRIB echo (open circles) and signal to noise ratio (plain triangles) as a function of the number of incident photons $\overline{n}$, for 200 ns input pulses. (b) CRIB echo for $\overline{n}$ = 0.6 (integration time 25000s). Dark counts have been subtracted from the data.

In the following we analyze the efficiency and storage time performances of our memory in more detail. Ref. [11] gives a simplified model for the CRIB memory. In this model, the storage and retrieval efficiency if the echo is emitted in the forward direction is given by :

$$\eta_{CRIB}(t) = d^2 e^{-d} e^{-t^2\tilde{\gamma}^2} \qquad (1)$$

where $\tilde{\gamma} = 2\pi\gamma$ is the spectral width (standard deviation) of the initial absorption peak, and d is the optical depth of the broadened absorption peak. The main assumption here is that the spectral width of the absorption peak is much wider than the spectral bandwidth of the photon to be stored. The first term may be interpreted as the collective interaction which depends on the square of the number of atoms in the absorption peak. The second factors describes the re-absorption of the emitted photons by the resonant atoms. Finally, the third term accounts for the decoherence due to the finite width of the initial absorption peak, assuming a gaussian spectral profile. By fitting

the decay curve of Fig. 3 with Eq. 1, we find a full width at half maximum linewidth of the central peak of 1MHz. This value corresponds well to the results obtained by a measurement of the transmission spectrum. The minimal width of this peak is limited by the linewidth of our unstabilized laser diode and power broadening during the preparation of the peak. The optical coherence time of the transition under our experimental conditions has been measured independently by photon echo spectroscopy. It was found to be $T_2 \approx 2\mu s$, which corresponds to a homogeneous linewidth of 160 kHz. Note that the optical coherence in Er^{3+}:Y_2SiO_5could be drastically increased using lower temperatures and higher magnetic fields [26].

In our experiment, imperfect optical pumping results in a large absorbing background with optical depth d_0, which acts as a passive loss, such that the experimental storage and retrieval efficiency is given by: $\eta(t) = \eta_{CRIB}(t)\exp(-d_0)$ [22]. The values of d and d_0 can be measured by recording the absorption spectra. This yields an optical depth of the unbroadened peak $d' = 0.5\pm0.2$ and an absorbing background of $d_0 = 1.6\pm0.1$. A voltage of 50 V on the electrodes corresponds to a broadening of a factor of $\sim$3 [39], leading to $d = 0.17 \pm 0.07$. In our experiment, the photon bandwidth is of the same order as the broadened peak, so that the assumptions of the simplified model are not fulfilled. In order to have a more accurate description, we have solved numerically the Maxwell-Bloch equations with the measured d', using a gaussian initial peak. This gives storage and retrieval efficiencies of order $1.5 \cdot 10^{-3}$ (including the passive loss d_0) for a storage time of 300 ns, in reasonable agreement with the measured values (see Fig. 3)

This study shows that the main reason of the low storage and retrieval efficiency in the present experiment is the small absorption in the broadened peak and the large absorbing background, due to imperfect optical pumping. About 80 % of the retrieved photons are lost in the absorbing background. The limited optical pumping efficiency is due to the small branching ratio in the lambda system and to the the short life time of the ground state Zeeman transition [30]. This may be improved in several ways: first, the branching ratio could be increased by spin mixing using RF fields in the excited state [30]. In order to increase the population lifetime of Zeeman levels, it might be interesting to work at higher magnetic field (hundreds of mT), in order to reduce spin-spin interactions. Other crystals might also be explored, e.g., Y_2O_3, to search for longer Zeeman lifetimes. Finally, it would also be interesting to investigate hyperfine states, which might have longer spin-population relaxation lifetimes.

In summary, we have presented a proof-of-principle of quantum memory for photons at telecommunication wavelengths. Pulses of light at the single photon level have been stored and retrieved in an Erbium doped crystal, using the CRIB protocol. Continuing efforts to increase the efficiency and the storage time will be required in order to build a useful device for applications in quantum information science. Our experiment is nevertheless an enabling step towards the demonstration of a fiber network compatible quantum light matter interface.

The authors acknowledge technical assistance by Claudio Barreiro and Jean-Daniel Gautier as well as stimulating discussions with Imam Usmani, Wolfgang Tittel, Sara Hastings-Simon, Matthias Staudt and Nino Walenta. This work was supported by the Swiss NCCR Quantum Photonics, by the European Commission under the Integrated Project Qubit Applications (QAP) and the ERC-AG Qore.

[1] K. Hammerer, A. Sorensen, and E. Polzik, arXiv:0807.3358 (2008).
[2] H.-J. Briegel, W. Dür, J. I. Cirac, and P. Zoller, Phys. Rev. Lett. **81**, 5932 (1998).
[3] L.-M. Duan, M. D. Lukin, J. I. Cirac, and P. Zoller, Nature **414**, 413 (2001).
[4] C. Simon *et al.*, Phys. Rev. Lett. **98**, 190503 (2007).
[5] N. Sangouard, C. Simon, H. de Riedmatten, and N. Gisin, arXiv:0906.2699 (2009).
[6] M. Fleischhauer and M. D. Lukin, Phys. Rev. Lett. **84**, 5094 (2000).
[7] A. E. Kozhekin, K. Mølmer, and E. Polzik, Phys. Rev. A **62**, 033809 (2000).
[8] S. A. Moiseev and S. Kröll, Phys. Rev. Lett. **87**, 173601 (2001).
[9] B. Kraus *et al.*, Phys. Rev. A **73**, 020302 (2006).
[10] J. Nunn *et al.*, Phys. Rev. A **75**, 011401 (2007).
[11] N. Sangouard, C. Simon, M. Afzelius, and N. Gisin, Phys. Rev. A **75**, 032327 (2007).
[12] M. Afzelius, C. Simon, H. de Riedmatten, and N. Gisin, Phys. Rev. A **79**, 052329 (2009).
[13] T. Chanelière *et al.*, Nature **438**, 833 (2005).
[14] M. D. Eisaman *et al.*, Nature **438**, 837 (2005).
[15] K. S. Choi, H. Deng, J. Laurat, and H. J. Kimble, Nature **452**, 67 (2008).
[16] K. Akiba, K. Kashiwagi, M. Arikawa, and M. Kozuma, New Journal of Physics **11**, 013049 (2009).
[17] B. Julsgaard *et al.*, Nature **432**, 482 (2004).
[18] J. Appel *et al.*, Phys. Rev. Lett. **100**, 093602 (2008).
[19] K. Honda *et al.*, Phys. Rev. Lett. **100**, 093601 (2008).
[20] J. Cviklinski *et al.*, Phys. Rev. Lett. **101**, 133601 (2008).
[21] A. D. Boozer *et al.*, Phys. Rev. Lett. **98**, 193601 (2007).
[22] H. de Riedmatten *et al.*, Nature **456**, 773 (2008).
[23] N. Sangouard *et al.*, Phys. Rev. A **76**, 050301 (R) (2007).
[24] N. Sangouard *et al.*, Phys.Rev.A **77**, 062301 (2008).
[25] T. Böttger, Y. Sun, C. W. Thiel, and R. L. Cone, Phys. Rev. B **74**, 075107 (2006).
[26] T. Böttger, C. W. Thiel, R. L. Cone, and Y. Sun, Phys. Rev. B **79**, 115104 (2009).
[27] E. Baldit *et al.*, Phys. Rev. Lett. **95**, 143601 (2005).
[28] M. U. Staudt *et al.*, Phys. Rev. Lett. **99**, 173602 (2007).
[29] M. U. Staudt *et al.*, Phys. Rev. Lett. **98**, 113601 (2007).

[30] B. Lauritzen *et al.*, Phys. Rev. A **78**, 043402 (2008).
[31] N. Kurnit, I. Abella, and S. Hartmann, Phys. Rev. Lett. **13**, 567 (1964).
[32] J. Ruggiero, J.-L. Le Gouët, C. Simon, and T. Chanelière, Phys. Rev. A **79**, 053851 (2009).
[33] A. L. Alexander, J. J. Longdell, M. J. Sellars, and N. B. Manson, Phys. Rev. Lett. **96**, 043602 (2006).
[34] W. Tittel *et al.*, Laser & Photonics Review 1 (2009).
[35] A. Alexander, J. Longdell, M. Sellars, and N. Manson, Journal of Luminescence **127**, 94 (2007).
[36] G. Hétet *et al.*, Phys. Rev. Lett. **100**, 023601 (2008).
[37] G. Hétet *et al.*, Opt. Lett. **33**, 2323 (2008).
[38] S. R. Hastings-Simon *et al.*, Phys. Rev. B **78**, 085410 (2008).
[39] J. Minář *et al.*, arXiv:0907.2344 (2009).
[40] G. N. Gol'tsman *et al.*, Appl. Phys. Lett. **79**, 705 (2001).